Vector-field LOS-based sliding mode path-following control with surge velocity constraints for underactuated surface vehicles under disturbances

Nguyen Trong Khuyen[1*], Cao Duc Sang[1], Ho Si Duong[1],
Vu Hai Ha[1], Nguyen Thi Le Quyen[2], Truong Tat Anh[3]

[1]Institute of Automation, Academy of Military Science and Technology, 89B Ly Nam De, Hoan Kiem, Hanoi, Vietnam;
[2]Nghe An University, 51 Ly Tu Trong, Vinh Phu, Nghe An, Vietnam;
[3]Institute of Mechanical Engineering and Dynamics, University of Transport Technology, 54 Trieu Khuc, Thanh Liet, Hanoi, Vietnam;
[*]Corresponding author: nguyentk126@gmail.com
Received 5 Jun. 2026; Revised 17 Aug. 2026; Accepted 04 Sep. 2026; Published 16 Sep. 2026.
DOI: https://doi.org/10.54939/1859-1043.j.mst.FMC.2026.209-218

ABSTRACT

This paper presents a constrained vector-field line-of-sight (VFLOS)-based sliding mode path-following control scheme for underactuated surface vessels subject to unknown disturbances. To enforce surge-velocity constraints, a hyperbolic tangent function is incorporated into the VFLOS guidance law, ensuring that the commanded surge velocity remains within predefined bounds. Based on the generated guidance commands, a sliding mode controller is developed to achieve accurate surge-velocity and heading tracking while providing robustness against unknown environmental disturbances. To suppress chattering in the control inputs, a first-order low-pass filter is incorporated at the controller output. Lyapunov stability analysis proves that all closed-loop signals remain bounded and that the path-following errors asymptotically converge to zero while satisfying the prescribed velocity constraints. Simulation results demonstrate that the proposed method achieves accurate and robust path-following under various disturbance conditions, while the low-pass filter effectively smooths the control inputs with negligible degradation in tracking performance. The proposed approach provides an effective solution for constrained path-following control of underactuated surface vessels operating in uncertain marine environments.

Keywords: Vector field line-of-sight guidance; Sliding mode control; Underactuated surface vehicles; Low-pass filter.

1. INTRODUCTION

The path-following problem for autonomous surface vehicles is an important topic in control and guidance, with applications in search and rescue, ocean exploration, maritime surveillance, and patrol missions. For surface vehicles, a three-degree-of-freedom dynamic model consisting of surge, sway, and yaw motions is commonly employed [2].

Extensive studies have been conducted on fully actuated vehicles [4]. However, the path-following problem for underactuated vehicles has attracted greater attention due to its closer correspondence to the practical structure of marine craft. At the kinematic level, guidance laws based on the Line-of-Sight (LOS) technique are widely adopted because of their simplicity and effectiveness. Nevertheless, in the conventional LOS guidance law [14], the along-track error ex is often neglected. In [5], the authors proposed a modified LOS scheme for Dubins paths combined with a sideslip-angle observer, ensuring uniform semiglobal asymptotic stability (USGAS) for the cross-track error ey. However, the convergence of the along-track error ex and the reference speed tracking problem were not considered. In [12], an Improved LOS guidance law combined with path-parameter control was proposed, ensuring convergence of the tracking errors to zero. Recent studies have also considered various constraints in LOS-based guidance for

underactuated surface vehicles. A constrained LOS guidance method was developed to handle output and input constraints, where a barrier Lyapunov function was employed in the guidance layer and model predictive control was used to address input saturation [1]. A cross-track error constraint was also incorporated into an LOS guidance algorithm for underactuated unmanned surface vehicles, providing bounded tracking errors while accounting for an unknown sideslip angle [3]. Furthermore, safety-certified LOS guidance was proposed to simultaneously consider surge-velocity and yaw-rate constraints in constrained water regions, where a quadratic programming framework was employed to generate feasible guidance commands [6].

At the dynamic control level, Sliding Mode Control (SMC) and backstepping techniques are widely employed to enhance robustness against disturbances and model uncertainties [1, 4, 7, 8, 12]. In [4], an adaptive SMC controller was proposed for fully actuated systems under the assumption that the upper bound of disturbances is known a priori. Other studies combined SMC with an Extended State Observer (ESO) to improve disturbance rejection capability for underactuated vehicles [9, 10]. From the perspective of optimal control, Model Predictive Control (MPC) has been applied to handle input constraints and improve path-following performance [1]; however, these approaches rely on linearized dynamic models. Several works employed adaptive backstepping methods to guarantee stability in the presence of parametric uncertainties [11], although disturbance rejection capability was not fully addressed [12].

This paper focuses on the path-following problem of underactuated surface vehicles with constrained surge velocity and unknown disturbances. The main contributions of this work are summarized as follows:

i. A vector-field LOS guidance law is developed to generate the desired heading while explicitly enforcing the prescribed surge-velocity constraints.

ii. A sliding mode controller is designed to achieve surge-velocity and heading tracking with robustness against unknown disturbances.

iii. A first-order low-pass filter is incorporated into the control loop to mitigate chattering with small degradation in tracking performance.

iv. The stability of the closed-loop system is established using Lyapunov analysis, and the effectiveness of the proposed method is verified through numerical simulations.

The paper is organized as follows. Section 2 presents the model and guidance–control design, while Section 3 presents the simulation results. Section 4 concludes the paper.

2. METHODOLOGY

2.1. Surface vehicle dynamics and tracking problem formulation

2.1.1. Underactuated surface vehicle dynamic

The paper employs a three-degree-of-freedom (3-DOF) dynamic model, including surge, sway, and yaw motions, to describe the surface vehicle dynamics [1].

$$\begin{cases} \dot{\eta} = R(\psi)\upsilon \\ M\dot{\upsilon} + C(\upsilon)\upsilon + D(\upsilon)\upsilon = \tau + \tau_d \end{cases} \tag{1}$$

Where $v = [u, \mathrm{v}, r]^T$: và $\eta = [x, y, \psi]^T$, u, v, and r denote the surge, sway, and yaw velocities, respectively; x and y represent the vehicle position in the inertial reference frame, and ψ is the heading angle. M, C, and D denote the inertia matrix, Coriolis–centripetal matrix, and damping matrix, respectively. τ, τ_d represent the control input and external disturbance, respectively. For an underactuated vehicle $\tau = [F, 0, T]^T$. Model (1) can be transformed into (2).

$$\begin{cases} \dot{u} = f_u(u,v,r) + b_u F + \delta_u \\ \dot{v} = f_v(u,v,r) + b_v T + \delta_v \\ \dot{r} = f_r(u,v,r) + b_r T + \delta_r \end{cases} \tag{2}$$

Where $f_u, f_v, f_r, b_u, b_v, b_r, \delta_u, \delta_v, \delta_r$ can be found on page 4 of [13].

2.1.2. Path following problems

The path is described as a function of the path parameter $P_d(\gamma):[a,b]\to R^2$, where γ is the path parameter varying over an interval $[a,b]$. When this parameter is parameterized with respect to time, i.e. $\gamma=\gamma(t)$, the reference point on the path is determined by $P_r = P_d(\gamma(t))$, thereby transforming the problem from a purely geometric formulation into a time-dependent one.

Define e - as the tracking error between the actual position of USV and the reference position:

$$e(t) \triangleq P_r - P_v = [e_x, e_y]^T \tag{3}$$

In the Frenet frame:

$$\begin{bmatrix} e_x \\ e_y \end{bmatrix} = \begin{bmatrix} \cos\psi_r & \sin\psi_r \\ -\sin\psi_r & \cos\psi_r \end{bmatrix} \begin{bmatrix} x - x_r \\ y - y_r \end{bmatrix} \tag{4}$$

$$\begin{aligned} \begin{bmatrix} \dot{e}_x \\ \dot{e}_y \end{bmatrix} &= \begin{bmatrix} \cos\psi_r & \sin\psi_r \\ -\sin\psi_r & \cos\psi_r \end{bmatrix} \begin{bmatrix} \dot{x} - \dot{x}_r \\ \dot{y} - \dot{y}_r \end{bmatrix} + \dot{\psi}_r \begin{bmatrix} -\sin\psi_r & \cos\psi_r \\ -\cos\psi_r & -\sin\psi_r \end{bmatrix} \begin{bmatrix} x - x_r \\ y - y_r \end{bmatrix} \\ &= R(-\psi_r)\left(R(\psi)R(\beta)\begin{bmatrix} U \\ 0 \end{bmatrix} - R(\psi_r)\begin{bmatrix} U_r \\ 0 \end{bmatrix} \right) + \dot{\psi}_r \begin{bmatrix} e_y \\ -e_x \end{bmatrix} \\ &= R(\psi + \beta - \psi_r)\begin{bmatrix} U \\ 0 \end{bmatrix} + \begin{bmatrix} -U_r + e_y\dot{\psi}_r \\ -e_x\dot{\psi}_r \end{bmatrix} \end{aligned} \tag{5}$$

Where $\psi_r = \arctan(v_r / u_r), \beta = \arctan(v/u)$, $U = \sqrt{u^2 + v^2}, U_r = \sqrt{\dot{x}_r^2 + \dot{y}_r^2}$.

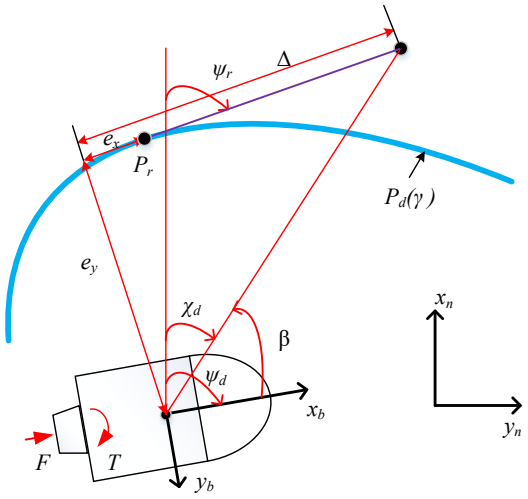


Figure 1. *Tracking errors expressed in the Frenet frame.*

$$\dot{e}_x = U\cos(\psi + \beta - \psi_r) - U_r + e_y\dot{\psi}_r = U\cos\alpha - U_r + e_y\dot{\psi}_r \tag{6}$$

$$\dot{e}_y = U\sin(\psi + \beta - \psi_r) - e_x\dot{\psi}_r = U\sin\alpha - e_x\dot{\psi}_r \tag{7}$$

Where $\alpha = \psi + \beta - \psi_r$, $\beta = \arctan(v/u)$, assuming that β is available from the vehicle velocity measurements, ψ_r - the tangent angle of the path at the reference point P_r. Assuming that the reference point moves with the desired velocity U_0, it follows that:

$$\dot{e}_x = U\cos(\psi + \beta - \psi_r) - U_0 + e_y\dot{\psi}_r = U\cos\alpha - U_0 + e_y\dot{\psi}_r \tag{8}$$

$$\dot{e}_y = U\sin(\psi + \beta - \psi_r) - e_x\dot{\psi}_r = U\sin\alpha - e_x\dot{\psi}_r \tag{9}$$

The control objective is formulated as follows:

$$\begin{cases} e_x \to 0, e_y \to 0 \\ U \to U_0 \end{cases}, \text{ when } t \to \infty \tag{10}$$

2.2. Vector-field LOS guidance law with surge velocity constraint

Assume that the desired heading angle ψ_d is designed such that:

$$U\cos\alpha = U_0 - k_x\tanh\left(\frac{e_x}{L_x}\right), U\sin\alpha = -k_y e_y \tag{11}$$

It follows that:

$$\alpha = \arctan\left(\frac{-k_y e_y}{U_0 - k_x\tanh\left(\frac{e_x}{L_x}\right)}\right) \tag{12}$$

Vector field-LOS guidance law is designed as:

$$\psi_d = \psi_r - \beta + \alpha = \psi_r - \beta + \arctan\left(\frac{-k_y e_y}{U_0 - k_x\tanh\left(\frac{e_x}{L_x}\right)}\right) \tag{13}$$

As $e_y \to 0$, $\alpha \to 0$, then $\cos\alpha \to 1$. Accordingly, the surge velocity is designed as:

$$u_d = U\cos\beta = \left(U_0 - k_x\tanh\left(\frac{e_x}{L_x}\right)\right)\cos\beta \tag{14}$$

Due to $\left|\tanh\left(e_x/L_x\right)\right| \le 1$, if we select the gain coefficient $k_x < U_0$, and it is assumed that $|\beta| < \beta_{\max} < \pi/2$. This assumption is consistent with normal operating conditions, where the sideslip angle is often small. Then u_d is bounded within the interval:

$$\left(U_0 - k_x\right)\cos\beta_{\max} \le u_d \le \left(U_0 + k_x\right)$$

Stability analysis:

Choose Lyapunov function: $V = \frac{1}{2}e_x^2 + \frac{1}{2}e_y^2$.

$$\begin{aligned} \dot{V} &= e_x\dot{e}_x + e_y\dot{e}_y = e_x\left(-k_x\tanh\left(e_x/L_x\right) + e_y\dot{\psi}_r\right) + e_y\left(-k_y e_y - e_x\dot{\psi}_r\right) \\ &= -k_x e_x\tanh\left(e_x/L_x\right) - k_y e_y^2 \end{aligned} \tag{15}$$

Here, we note that: $e_x \tanh\left(e_x / L_x\right) \geq 0, \forall e_x$. Then $\dot{V} < 0$, the guidance subsystem is asymptotically stable under $u = u_d, \psi = \psi_d$. Consequently, $e_x \to 0, e_y \to 0$.

2.3. Dynamic controller design

The control problem is reduced to designing the control force F and control moment T such that the USV tracks the desired heading angle ψ_d and desired surge velocity u_d defined in (13) and (14), respectively. Consider the surge dynamics: $\dot{u} = f_u + b_u F + \delta_u$.

Let $e_u = u - u_d$, it holds that: $\dot{e}_u = \dot{u} - \dot{u}_d = f_u + b_u F + \delta_u - \dot{u}_d$.

Where: $\dot{u}_d = -k_x \left[1 - \tanh^2\left(e_x / L_x\right)\right] \frac{\dot{e}_x}{L_x} \cos\beta - \left[U_d - k_x \tanh\left(e_x / L_x\right)\right] \sin\beta \frac{u\dot{v} - \dot{u}v}{u^2 + v^2}$.

The force control law is designed as:

$$F = \frac{1}{b_u}\left(-k_u e_u - f_u + \dot{u}_d - \bar{\delta}_u \operatorname{sgn}(e_u)\right) \tag{16}$$

Here $\bar{\delta}_u$ is positive constant, $\bar{\delta}_u \geq \sup\{\delta_u\}$. Choose the Lyapunov function as: $V_1 = \frac{1}{2} e_u^2$.

$$\dot{V}_1 = e_u \dot{e}_u = e_u \left(f_u + (-k_u e_u - f_u + \dot{u}_d - \bar{\delta}_u \operatorname{sgn}(e_u)) + \delta_u - \dot{u}_d\right) = -k_u e_u^2 - (\bar{\delta}_u |e_u| - \delta_u e_u) < 0$$

According to Lyapunov stability theory, it follows that: $e_u \to 0$, or $u \to u_d$ as $t \to \infty$.

Next, consider the yaw dynamics: $\begin{cases} \dot{\psi} = r \\ \dot{r} = f_r + b_r T + \delta_r \end{cases}$

Let: $e_\psi = \psi - \psi_d$, $\dot{e}_\psi = r - \dot{\psi}_d$. Choose sliding surface:

$$s_\psi = \dot{e}_\psi + \lambda e_\psi = r - \dot{\psi}_d + \lambda e_\psi, \text{ với } \lambda > 0 \tag{17}$$

$$\dot{s}_\psi = \dot{r} - \ddot{\psi}_d + \lambda \dot{e}_\psi = f_r + b_r T + \delta_r - \ddot{\psi}_d + \lambda \dot{e}_\psi \tag{18}$$

The moment control law design:

$$T = \frac{1}{b_r}\left(-k_\psi s_\psi - f_r + \ddot{\psi}_d - \lambda \dot{e}_\psi - \bar{\delta}_r \operatorname{sgn}(s_\psi)\right) \tag{19}$$

Where $\bar{\delta}_r$ - positive constant, $\bar{\delta}_r \geq \sup\{\delta_r\}$. Let the Lyapunov function:

$$V_2 = \frac{1}{2} s_\psi^2$$

$$\begin{aligned} \dot{V}_2 &= s_\psi \dot{s}_\psi = s_\psi \left(f_r + (-k_\psi s_\psi - f_r + \ddot{\psi}_d - \lambda \dot{e}_\psi - \bar{\delta}_r \operatorname{sgn}(s_\psi)) + \delta_r - \ddot{\psi}_d + \lambda \dot{e}_\psi\right) \\ &= -k_\psi s_\psi^2 - (\bar{\delta}_r |s_\psi| - \delta_r s_\psi) < 0 \end{aligned}$$

According to the Lyapunov stability theory, it follows that: $s_\psi \to 0$, or $\dot{e}_\psi + \lambda e_\psi \to 0$. Since $\lambda > 0$, the sliding surface dynamics is exponentially stable. Therefore $e_\psi \to 0$ as $t \to \infty$.

Therefore, (16) and (19) ensure the asymptotic convergence of the surge velocity and heading angle to their desired values. Since the control errors u - u_d and ψ - ψ_d asymptotically converge to zero, their effects on the guidance subsystem vanish asymptotically. Assuming that the desired guidance signals and their required derivatives are bounded, the guidance and control subsystems form an asymptotically stable cascade. Consequently, e_x, $e_y \to 0$, u - $u_d \to 0$, ψ - $\psi_d \to 0$.

2.4. Control input smoothing using a low-pass filter

Although the proposed SMC controller has been proven to be Lyapunov stable, the switching term based on the sign(·) function still induces high-frequency oscillations (chattering) in the thrust force F and control moment T, degrading the control signal quality and potentially affecting the actuators. To mitigate this phenomenon, a first-order low-pass filter (LPF) is introduced at the controller output with the following transfer function:

$$G_f(s) = \frac{\omega_c}{s + \omega_c} \tag{20}$$

Where ω_c is the cutoff frequency. The filtered control inputs applied to the actuators are

$$\begin{cases} F_f(s) = G_f(s)F(s) \\ T_f(s) = G_f(s)T(s) \end{cases} \tag{21}$$

Where F_f và T_f are the filtered control inputs applied to the actuators.

The first-order low-pass filter is a stable dynamic subsystem. Its use for chattering attenuation while preserving stability has been established in previous studies [15, 16]. Under bounded reference signals and their derivatives, the filtering error remains bounded and can be treated as a bounded perturbation to the guidance–control subsystem. Therefore, based on the standard cascade/ISS stability framework, the complete closed-loop system with the low-pass filter is uniformly ultimately bounded (UUB).

In this study, the cutoff frequency is selected as $\omega_c = 5\ rad/s$ based on simulation and control performance evaluation. The simulation results demonstrate that the proposed filter significantly reduces the chattering of the thrust force and control moment while maintaining the convergence and path-following performance of the vehicles.

3. SIMULATION AND DISCUSSION

In the simulation, the surface vehicle parameters are selected as m_{11} = 200 kg; m_{22} = 300 kg; m_{33} = 200 kg.m^2; $m_{23} = m_{32}$ = 20 kg.m; d_{11} = 70 kg/s; d_{22} = 100 kg/s; d_{33} = 50 kg.m^2/s; $d_{23} = d_{32}$ = -30 kg.m/s; $c_1 = m_{11}$; $c_2 = m_{22}$; $c_3 = m_{23}$. The desired trajectory is given by P_d = [100cos(0.5γ), 100sin(0.5 γ)]^T, γ(0) = 0. The disturbance vector is selected as $\tau = [30 * sin(0.5 * t), 10 * cos(t), 10 * sin(0.5 * t)]^T$. The desired surge velocity is chosen as U_0 = 1 m/s. The simulation results are compared with those of the controllers constrained LOS (CLOS) [1] and LOS-BS in [12].

The simulation results show that the proposed method provides strong disturbance-rejection capability. In both disturbed and disturbance-free cases, the vehicle asymptotically converges to the reference trajectory, with e_x and e_y approaching zero (Figures 4-7), while satisfying the surge-velocity constraint of [0.90, 1.05] m/s (Figure 9). In contrast, CLOS-SMC [1] and LOS-BS [12] exhibit poorer disturbance rejection, with e_y oscillating and failing to converge to zero under disturbances (Figures 4, 5), despite the rapid convergence of e_x (Figures 6, 7). Furthermore, the introduction of the low-pass filter has a negligible impact on the path-following performance while significantly reducing the oscillations of the control inputs, resulting in smoother thrust force and control moment.

Figure 8 shows that, under the proposed method, the USV heading tracks the desired heading. It also shows that the sideslip angle remains below the prescribed bound β_{max} = 0.2 rad throughout the simulation.

The quantitative results in Tables 1 and 2 provide a comprehensive comparison of the tracking performance. For the along-track error e_x, LOS-BS achieves a lower RMSE than VFLOS-SMC (0.191 versus 0.783), indicating a smaller overall error magnitude. However, its ITAE is

substantially higher (1743.9 versus 473.4), suggesting slower error attenuation and a longer transient response. For the cross-track error e_y, the two methods exhibit comparable RMSE values (1.957 for LOS-BS versus 1.789 for VFLOS-SMC), whereas VFLOS-SMC yields a markedly lower ITAE (599.8 versus 4458.4). This indicates that the proposed method achieves faster attenuation of the cross-track error and better transient performance.

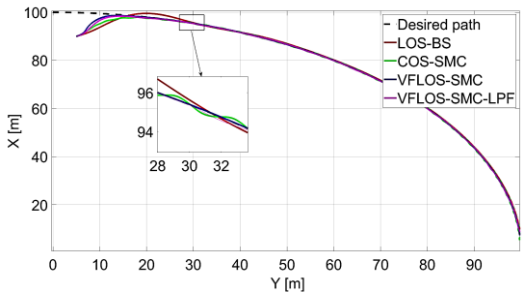


Figure 2. *Trajectories without disturbances.*

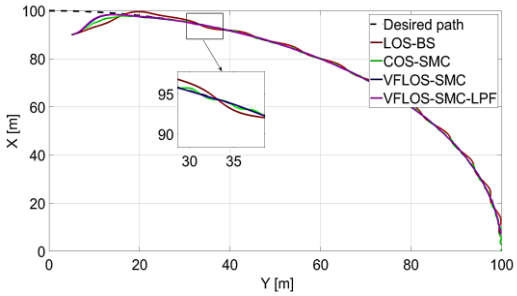


Figure 3. *Trajectories under disturbances.*

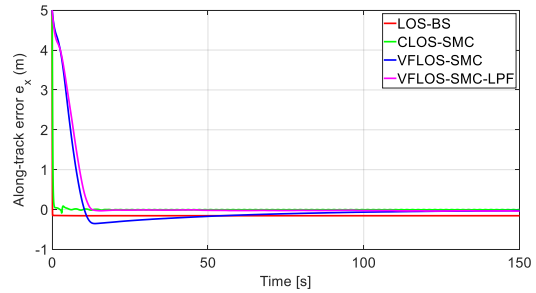


Figure 4. *Along-track error without disturbances.*

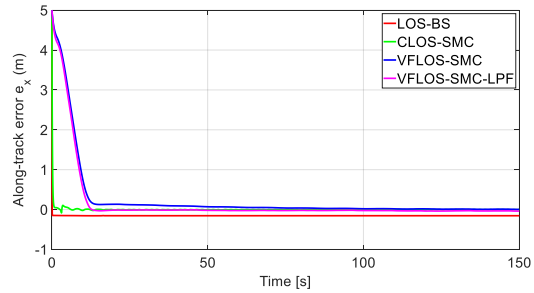


Figure 5. *Along-track error under disturbances.*

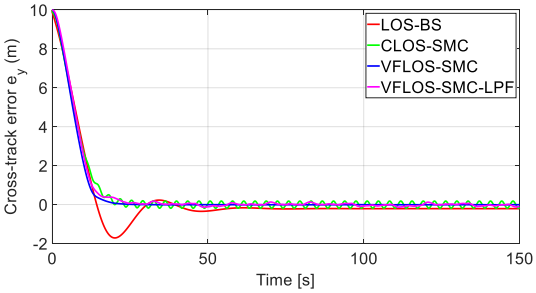


Figure 6. *Cross-track error without disturbances.*

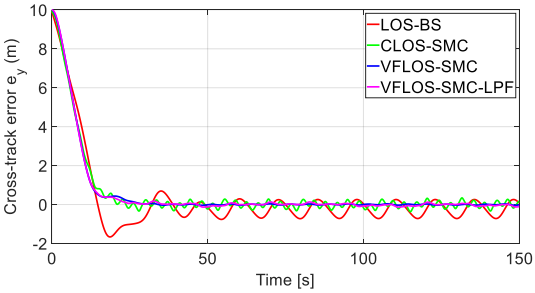


Figure 7. *Cross-track error under disturbances.*

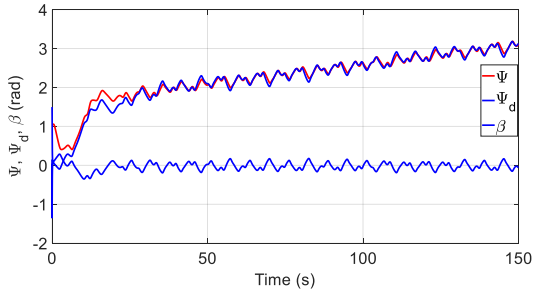


Figure 8. *Yaw and sideslip under disturbances.*

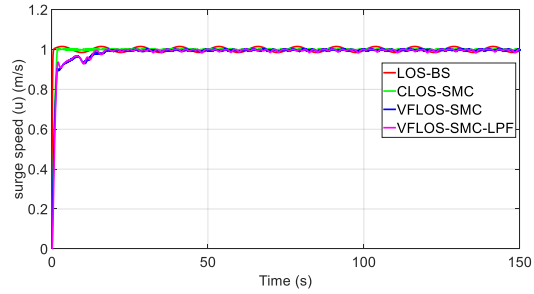


Figure 9. *Surge speeds of USV under disturbances.*

Table 1. *Comparison between the proposed controller and LOS-BS without disturbances.*

	VFLOS-SMC			VFLOS-SMC-LPF		LOS-BS		CLOS-SMC	
	e_x	e_y	u	e_x	e_y	e_x	e_y	e_x	e_y
RMSE	0.801	1.843	0.992	0.7895	1.865	0.191	1.870	0.118	1.819
ITAE	141.7	424.6	11244	366.7	1493	1743.7	2966.3	44.9	1652

Table 2. *Comparison between the proposed controller and LOS-BS under disturbances.*

	VFLOS-SMC			VFLOS-SMC-LPF		LOS-BS		CLOS-SMC	
	e_x	e_y	u	e_x	e_y	e_x	e_y	e_x	e_y
RMSE	0.783	1.789	0.991	0.798	1.862	0.191	1.957	0.118	1.835
ITAE	473.4	599.8	11205	414.3	921.1	1743.9	4458.4	48.6	1829

For CLOS-SMC [1], although e_x converges faster than with the proposed method, noticeable oscillations remain in e_y under both disturbed and disturbance-free conditions. This indicates that a faster along-track convergence does not necessarily translate into improved overall path-following performance. Overall, the comparable RMSE values, together with the substantially lower ITAE values achieved by VFLOS-SMC, demonstrate its improved transient performance, particularly in terms of cross-track error attenuation.

The RMSE and ITAE indices obtained with and without the LPF are also very similar for e_x, e_y, indicating that the LPF has a negligible effect on the path-following performance.

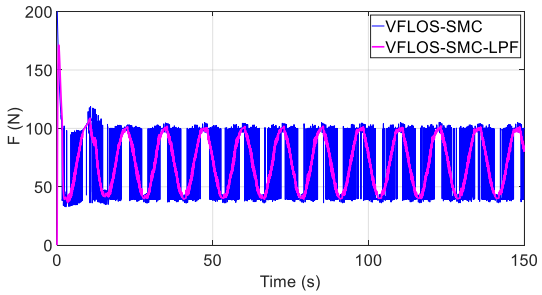


Figure 10. *Control force.*

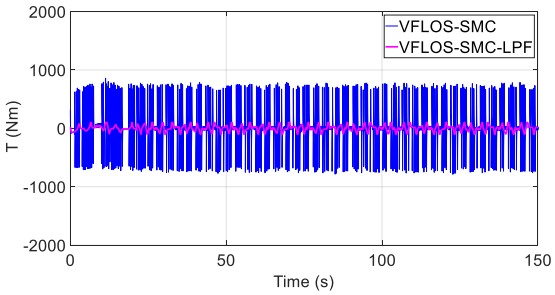


Figure 11. *Control moment.*

The control force and control moment under disturbance conditions are shown in Figure 10 and 11. The effect of the low-pass filter (LPF) is most evident in these control signals. The RMS values of the control force are reduced from 77.2 N (VFLOS-SMC) to 74.7 N (VFLOS-SMC-LPF), while the RMS values of the control moment are significantly reduced from 242.1 Nm to 50.4 Nm, respectively. Moreover, the LPF effectively smooths the control force and control moment by suppressing high-frequency oscillations. These results demonstrate that the LPF substantially reduces chattering and the oscillation amplitude of the control inputs without modifying the control law or degrading the path-following performance.

4. CONCLUSIONS

This paper proposed a vector-field LOS guidance law with surge-velocity constraints for USV path-following, together with a sliding-mode controller for surge-velocity and heading

tracking. By incorporating a hyperbolic tangent function into the guidance law, the commanded surge velocity was guaranteed to remain within predefined bounds. Furthermore, Lyapunov-based stability analysis proved the asymptotic convergence of USV. To suppress the chattering phenomenon induced by the switching control term, a first-order low-pass filter was introduced at the controller output, resulting in significantly smoother control inputs without degrading the path-following performance. Simulation results demonstrated the effectiveness of the proposed method in achieving accurate path-following performance while satisfying the prescribed velocity constraints. Comparative studies showed that the proposed method outperformed the CLOS-SMC and LOS-BS approaches, particularly in terms of disturbance rejection capability. The present study is limited to simulation-based validation, assumes bounded environmental disturbances, and does not explicitly consider actuator input saturation. Future work will focus on experimental validation under realistic marine conditions and on addressing actuator saturation and practical constraints.

REFERENCES

[1]. C. Liu, T. Sun and X. Wang, "*Constrained LOS guidance for path following of underactuated marine vehicle with input saturation*", Ocean Engineering, Vol. 307, p. 118217, (2024).

[2]. T. I. Fossen, "*Handbook of Marine Craft Hydrodynamics and Motion Control*", John Wiley & Sons, (2011).

[3]. H. Tong et al., "*Constrained control using novel nonlinear mapping for underactuated unmanned surface vehicles with unknown sideslip angle*", ISA Transactions, Vol. 141, (2023).

[4]. N. H. Quang, "*Robust adaptive path following controllers for autonomous surface vehicles with unknown disturbances*", Smart Systems and Devices, Vol. 34, No. 3, pp. 43–51, (2024).

[5]. T. I. Fossen et al., "*Line-of-sight path following for Dubins paths with adaptive sideslip compensation of drift forces*", IEEE Transactions on Control Systems Technology, (2014).

[6]. Z. Peng et al., "*Safety-certificated line-of-sight guidance of unmanned surface vehicles for straight-line following in a constrained water region subject to ocean currents*", Journal of Marine Science and Application, Vol. 22, No. 3, pp. 602–613, (2023).

[7]. Y. Wang, Y. Qu, S. Zhao, R. Cajo and H. Fu, "*Smooth sliding mode control for path following of underactuated surface vehicles based on LOS guidance*", Journal of Marine Science and Engineering, Vol. 11, No. 12, p. 2214, (2023).

[8]. H. Zhang, X. Zhang and R. Bu, "*Sliding mode adaptive control for ship path following with sideslip angle observer*", Ocean Engineering, Vol. 251, p. 111106, (2022).

[9]. T. Elmokadem, M. Zribi and K. Youcef-Toumi, "*Trajectory tracking sliding mode control of underactuated AUVs*", Nonlinear Dynamics, Vol. 84, pp. 1079–1091, (2016).

[10]. M. Li, C. Guo and H. Yu, "*Extended state observer-based integral line-of-sight guidance law for path following of underactuated unmanned surface vehicles with uncertainties and ocean currents*", International Journal of Advanced Robotic Systems, Vol. 18, No. 3, (2021).

[11]. A. P. Aguiar and J. A. P. Hespanha, "*Trajectory tracking and path-following of underactuated autonomous vehicles with parametric modeling uncertainty*", IEEE Transactions on Automatic Control, Vol. 52, No. 8, pp. 1362–1379, (2007).

[12]. T. Liu, Z. Dong, H. Du, L. Song and Y. Mao, "*Path following control of the underactuated USV based on the improved line-of-sight guidance algorithm*", Polish Maritime Research, Vol. 24, No. 1 (93), pp. 3–11, (2017).

[13]. D. S. Cao, K. N. Trong, H. H. Vu and A. T. Nguyen, "*A smooth robust controller for the path following of underactuated surface vehicles under disturbances*", JMST's Section on Computer Science and Control Engineering, No. CSCE9, pp. 3–12, (2025).

[14]. A. M. Lekkas and T. I. Fossen, "*Line-of-sight guidance for path following of marine vehicles*", Advanced in Marine Robotics, Vol. 5, pp. 63–92, (2013).

[15]. Swaroop et al., "*Dynamic surface control of nonlinear systems*", Proceedings of the 1997 American Control Conference, Vol. 5, IEEE, (1997).

[16]. D. Zhao, C. Li and Q. Zhu, "*Low-pass-filter-based position synchronization sliding mode control for multiple robotic manipulator systems*", Proceedings of the Institution of Mechanical Engineers, Part I: Journal of Systems and Control Engineering, Vol. 225, No. 8, pp. 1136–1148, (2011).

TÓM TẮT

Điều khiển bám đường dựa trên chế độ trượt và luật dẫn VFLOS có ràng buộc vận tốc tiến cho tàu mặt nước thiếu cơ cấu chấp hành dưới tác động của nhiễu bất định

Bài báo đề xuất một phương pháp điều khiển bám đường bằng chế độ trượt dựa trên luật dẫn đường trường vectơ VFLOS có ràng buộc vận tốc tiến cho tàu mặt nước thiếu cơ cấu chấp hành chịu tác động của nhiễu không xác định. Để bảo đảm ràng buộc vận tốc tiến, hàm hyperbolic tangent được tích hợp vào luật dẫn đường VFLOS nhằm duy trì vận tốc tiến tham chiếu trong các giới hạn định trước. Trên cơ sở các tín hiệu dẫn đường, bộ điều khiển chế độ trượt được thiết kế để bảo đảm khả năng bám chính xác vận tốc tiến và góc hướng. Để giảm hiện tượng chattering của tín hiệu điều khiển, một bộ lọc thông thấp bậc nhất được bổ sung tại đầu ra của bộ điều khiển nhằm làm mượt lực đẩy và mô-men điều khiển. Phân tích ổn định theo Lyapunov chứng minh rằng mọi tín hiệu trong hệ kín đều bị chặn và các sai số bám đường hội tụ tiệm cận về không trong khi vẫn thỏa mãn các ràng buộc vận tốc đặt trước. Kết quả mô phỏng xác nhận tính hiệu quả và tính bền vững của phương pháp đề xuất dưới các điều kiện nhiễu khác nhau. Đồng thời, bộ lọc thông thấp giúp giảm đáng kể dao động của tín hiệu điều khiển mà ít làm suy giảm chất lượng bám đường. Phương pháp đề xuất cung cấp một giải pháp hiệu quả cho bài toán điều khiển bám đường có ràng buộc đối với tàu mặt nước thiếu cơ cấu chấp hành hoạt động trong môi trường biển bất định.

Từ khoá: Luật dẫn đường véc tơ LOS; Điều khiển trượt; Tàu mặt nước thiếu dẫn động ; Bộ lọc thông thấp.